THE ASTROPHYSICAL JOURNAL, 443:341–347, 1995 April 10

DETECTION OF THE A1742−294 X-RAY BURSTER ABOVE 35 keV

E. CHURAZOV, M. GILFANOV, R. SUNYAEV, B. NOVICKOV, I. CHULKOV, V. KOVTUNENKO, A. SHEIKHET, AND K. SUKHANOV
Space Research Institute, Russian Academy of Sciences, Profsoyuznaya 84/32, 117810 Moscow, Russia
A. GOLDWURM, B. CORDIER, J. PAUL, AND P. O. PETRUCCI
Service d'Astrophysique, Centre d'Etudes Nucléaires de Saclay, 91191 Gif-sur-Yvette Cedex, France
AND
E. JOURDAIN, J. P. ROQUES, L. BOUCHET, AND P. MANDROU
Centre d'Etude Spatiale des Rayonnements, 9, avenu du Colonel Roche, BP 4346, 31029 Toulouse Cedex, France
Received 1994 February 28; accepted 1994 October 10

ABSTRACT

A transient hard state of the A1742−294 X-ray burster was detected by *Granat*/SIGMA in the course of 1992 fall observations of the Galactic center (GC) region. During the previous five sets of GC observations in 1990–1992, the flux above 35 keV was below the SIGMA detection limit. The spectrum observed in 1992 fall in the 35–200 keV band can be approximated by the emission of optically thin plasma with temperature $T_e \sim 40$ keV, much higher than $T_e \sim 8$ keV derived from the observations in the standard X-ray band by *Granat*/ART-P in 1990. Nevertheless, the spectrum of A1742−294 remains significantly softer than that of the nearby black hole candidate 1E 1740.7−2942.

Subject headings: stars: individual (A1742−294) — X-rays: bursts — X-rays: stars

1. INTRODUCTION

A1742−294, located ≈30′ from Sgr A*, is known as the brightest persistent source in the standard (2–20 keV) X-ray band in the 1° vicinity of the Galactic center. It was observed below 30 keV by *Ariel 5* (Wilson et al. 1977; Proctor et al. 1978), *SAS 3* (Jernigan et al. 1978), the *Einstein* IPC (Watson et al. 1981), Spacelab 2 (Skinner et al. 1987), Spartan 1 (Kawai et al. 1988), *Mir-Kvant* (Sunyaev et al. 1991b), and *Granat*/ART-P (Sunyaev et al. 1991a). Three bursts from this region have been observed by *SAS 3* (Lewin et al. 1976). The ART-P telescope firmly identified about a dozen X-ray bursts with A1742−294 (Pavlinsky et al. 1994). The spectrum in the standard X-ray band observed by ART-P can be approximated by the emission of optically thin plasma with temperature ≈8 keV (Pavlinsky et al. 1994).

2. THE INSTRUMENT AND OBSERVATIONS

Since the end of 1989, the *Granat Observatory* has been successfully operating on a highly eccentric orbit with a period of 4 days. The SIGMA coded mask telescope (Paul et al. 1991) on board *Granat*, with a NaI position-sensitive detector (Anger camera principle), provides sky images in the energy range 35–1300 keV with an angular resolution of approximately 15′. The instrument field of view (FOV) at the half-sensitivity boundary is an 11°.4 × 10°.5 rectangle. The region of the Galactic center has been observed by *Granat* in 1990–1992 in the spring and fall of each year. In most of the observations A1742−294 was located within the totally coded FOV of SIGMA, having maximum sensitivity.

3. THE IMAGES

For each energy channel, accumulated detector images with pixel size ∼3′.23 (4 times smaller than the angular size of the mask element) are stored on board. Sky images are reconstructed from the detector images via cross-correlations with the mask pattern. Contributions from opaque and transparent pixels are weighted with coefficients close to unity in order to produce a sky image equal to zero for a flat detector (for a discussion of image reconstruction techniques see, e.g., Fenimore & Cannon 1981). Prior to reconstruction, the recorded detector image D is corrected for the nonuniformity of the background in two steps. First of all, the detector image accumulated during the observations of source-free regions is subtracted ($D' = D - B$). Then, in order to remove residual nonuniformity of the background, the smoothed image of the detector is subtracted ($D'' = D' - D'_{\rm smoothed}$). Smoothing is done with a sliding window of size ∼2°. After cross-correlations, sky images obtained in individual observations are coaligned, coadded, and convolved with the point-spread function of the telescope in order to increase the sensitivity for the detection of point sources.

Shown in Figure 1 are the 3°.2 × 3°.2 slices of the SIGMA image in the 35–75 keV band near the position of 1E 1740.7−2942 obtained in 1992 fall. Although the peak (having a significance of ≈19 σ at maximum) is well centered on 1E 1740.7−2942 (Fig. 1*a*), the contours at lower intensity levels are clearly elongated toward the lower left side of the image. Subtracting the contribution of 1E 1740.7−2942 (Fig. 1*b*), we obtained the 5.8 σ peak close to the position of A1742−294. The best-fit position of the peak on the image (Fig. 1*b*) is R.A. = 265°.680, decl. = −29°.485 (1950), with a 90% error circle radius of 5′, and deviates from the position obtained by the *Einstein Observatory* (Watson et al. 1981) by 2′.4.

Because of the proximity of the weak source (A1742−294) to the bright source (1E 1740.7−2942), the detection of the former requires further justification.

3.1. *Contribution of 1E 1740−2942 to the A1742−294 Flux*

Although it is not apparent from the images convolved with the point-spread function (Fig. 1), the separation of these two

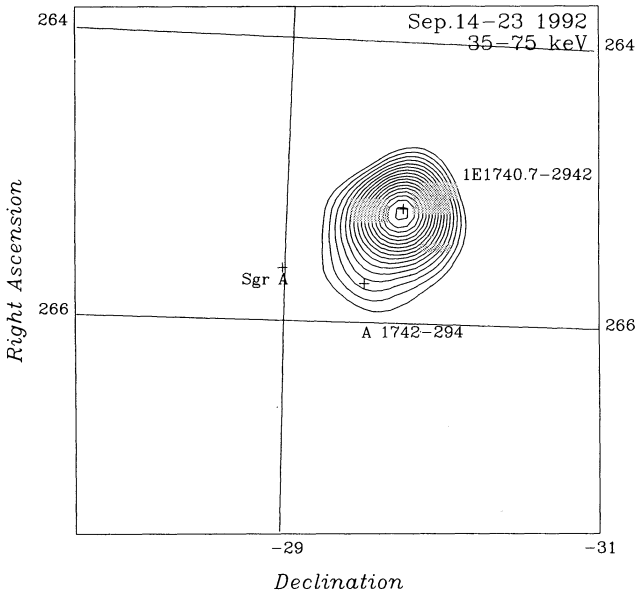

FIG. 1a

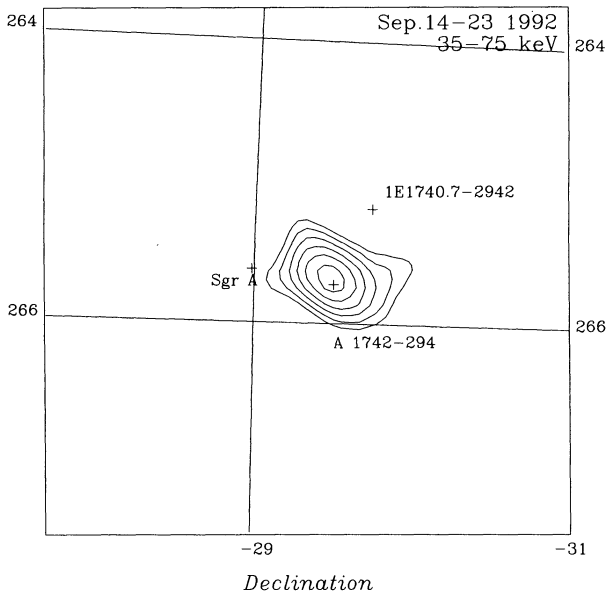

FIG. 1b

FIG. 1.—3°.2 × 3°.2 slice of the SIGMA 35–75 keV image near the position of 1E 1740.7−2942 obtained in 1992 fall. (*b*) Same image, but the contribution from 1E 1740.7−2942 has been subtracted. Contour levels are in standard deviations: (*a*) 3, 4, 5, 6, ..., 20 σ and (*b*) 3, 3.5, 4, ... σ. Crosses mark the positions of Sgr A, 1E 1740.7−2942, and A1742−294.

sources (~30′) is large enough to exclude strong mutual contamination of fluxes. Shown in Figure 2 (*middle and lower panels*) are the profiles of the images shown in Figure 1 along the line connecting 1E 1740.7−2942 and A1742−294. For comparison, in the upper panel, a similar profile of the image containing the bright X-ray source GRO 0422+32 is also shown. Thin lines in each panel show expected profiles. One can see that the expected contribution from 1E 1740.7−2942 is slightly negative at the A1742−294 position. The reason for negative wings of the profiles (~30′–50′ apart from the source) is the subtraction of the smoothed detectors prior to reconstruction (see above). Note also that during the observations in 1990 no strong positive flux was found at the A1742−294 position (Table 1), although 1E 1740.7−2942 was as bright as in 1992 fall. We concluded that the contribution from 1E 1740.7−2942 cannot explain the excess found at the A1742−294 position.

Although it is clear from Figure 2 that mutual contamination of 1E 1740.7−2942 and A1742−294 fluxes is weak, their spectra have been calculated by fitting the detector images in the given energy channel using the model consisting of expected illuminations from 1E 1740.7−2942 and A1742−294 and background. The fluxes from each source and background count rate were allowed to vary independently.

TABLE 1

FLUXES IN 35–100 keV RANGE OBTAINED FROM A1742−294 BY SIGMA DURING DIFFERENT PERIODS[a]

Period	Dates (MJD)	Exposure (s)	Flux (mcrab)
1990 spring.....	47,974.7–47,990.5	210,694.5	−2.7 ± 5.7
1990 fall	48,150.6–48,183.2	349,955.6	8.8 ± 3.9
1991 spring.....	48,309.4–48,330.5	335,088.1	6.0 ± 4.3
1991 fall	48,531.3–48,540.3	256,014.5	4.7 ± 5.0
1992 spring.....	48,670.6–48,721.7	910,236.5	−2.1 ± 2.6
1992 fall	48,879.5–48,888.2	374,465.9	30.9 ± 5.4
1993 spring.....	49,035.6–49,093.5	1,051,256.3	−0.4 ± 3.3

[a] Only observations obtained when the source was illuminating more than 70% of the detector area were used.

3.2. *Statistical and Systematic Errors*

The analysis described below has been performed in order to exclude the possibility of appearance of the peak at the A1742−294 position due to statistical or systematic errors. The contributions of 1E 1740.7−2942 and A1742−294 with expected profiles (Fig. 2) and estimated fluxes have been subtracted from the 35–75 keV image. The resulting image has been verified from the point of view of statistical quality. The ~4° × 4° totally coded FOV region has been used for this analysis. Root mean square variation of the fluxes measured in individual pixels on the final 35–75 keV image only by ~10% exceeds the value expected for pure statistical noise. Assuming that this excess can be attributed to the non-perfect correction for the nonuniformity of the background, all errors in the flux estimations should be increased by 10%. This translates to the reduction of the significance of the A1742−294 detection from 5.8 σ to $\approx$5.2 σ. Shown in Figure 3 is the distribution of fluxes (expressed in standard deviations) measured in individual pixels in the total coded FOV region. A 10% increase of errors in flux estimation has been taken into account. The thin line shows the expected shape of the distribution: it is Gaussian with zero mean and unit dispersion. There is no evidence for extended wings of the observed distribution which could indicate additional distortion of the image due to the systematic errors. the arrow shows the significance of A1742−294 detection (~5.2 σ).

Note that because of the convolution with the point-spread function the fluxes measured in the nearby pixels are not independent, although the shape of the distribution (Fig. 3) is described by a simple Gaussian. Monte Carlo simulations have been performed in order to estimate the probability of finding the 5.2 σ peak due to statistical fluctuations. In the course of

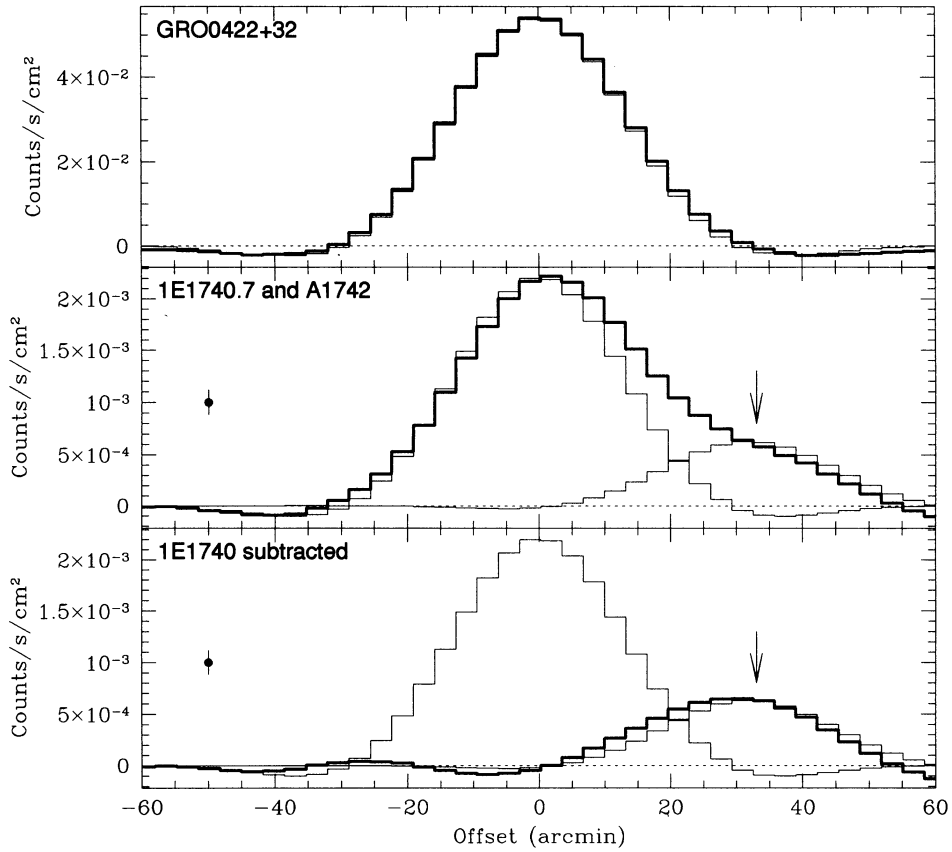

FIG. 2.—Profiles of images shown in Fig. 1 along the line connecting the positions of 1E 1740.7−2942 and A1742−294 (*thick lines*). A profile of the image with GRO 0422+322 is shown for comparison in the upper panel. The position of A1742−294 is shown by the arrow (1E 1740.7−2942 and GRO 0422+322 positions correspond to zero offset). Thin lines show the expected profiles for the sources with fluxes obtained in our analysis. In the lower panel, the contribution from 1E 1740.7−2942 has been subtracted. The histograms are given with 3′.23 resolution corresponding to the angular size of the detector pixel. At the left the error bars for individual points are shown. Note that individual points are not independent because of the convolution with the point-spread function.

simulations, 10^5 detector images (without sources) have been generated, and the whole reconstruction procedure has been applied. Only seven of the 10^5 images were found to contain peaks above 5.2 σ. Therefore, the probability of finding the $\gtrsim 5.2\ \sigma$ peak (somewhere on the image!) is $\sim 7 \times 10^{-5}$. The probability that the peak will be located within a few arcminutes of a given X-ray source (i.e., A1742−294) is much lower.

3.3. *Attitude Reconstruction Errors*

During each observation the pointing direction of the telescope axis varies by 20′–40′. This value is comparable to the separation between 1E 1740.7−2942 and A1742−294, and the possible contribution of 1E 1740.7−2942 to the flux measured at the position of A1742−294 due to the errors in attribute reconstruction should be discussed.

At the beginning of each session the star tracker of the telescope produces the map of the $\sim 7° \times 10°$ region with a resolution of $\sim 1'$. In each of five considered observations the star tracker detected from six to 15 bright stars. These stars have been identified with bright catalog objects with rms deviation from the expected positions of $\sim 0'.5$. On-board software selects two bright stars located on opposite sides of the star tracker field of view, and during the rest of the observation the positions of these two stars are measured each 4 s with accuracy better than $\sim 20''$. On-board software uses this information in order to correct the coordinates of X-ray photons for the variations of pointing direction. The distance between positions of these two stars given by the star tracker during each of the considered observations remained constant within $\sim 6''$ (rms). This value characterizes the uncertainty of measuring the coordinates of the stars by the star tracker and therefore characterizes the accuracy of the on-board reduction to single pointing. Numerous observations of the bright sources by *Granat*/SIGMA have shown that for the sessions with comparable quality of the star tracker data the accuracy of absolute pointing reconstruction is at least better than 1′. From Figure 2 one can see that uncertainties $\approx 1'$ do not affect measured fluxes because the width of the point-spread function is much larger.

We concluded that it is unlikely that detection of the peak at the position of A1742−294 could be due to the contribution from 1E 1740.7−2942, statistical and systematic errors, or attitude reconstruction error.

4. THE SPECTRUM AND VARIABILITY

Shown in Figure 4 (see also Table 1) are the fluxes in the 35–100 keV range measured by SIGMA during different periods of observation. Only sessions when the source was illuminating more than 70% of the detector area have been used. Several sessions where more complicated analysis is required (for example, due to the influence of strong solar flares on the detector background) have been excluded from the

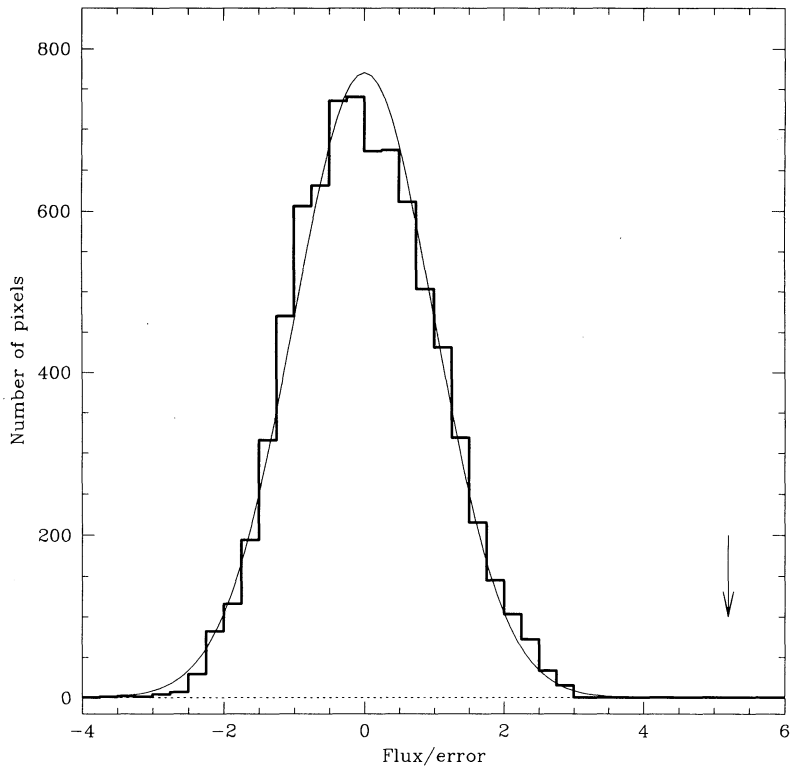

FIG. 3.—Distribution of fluxes (in standard deviations, increased by 10%) measured in individual pixels in the $\sim 4° \times 4°$ totally coded FOV region. Contributions of 1E 1740.7−2942 and A1742−294 have been subtracted from the image. The thin line shows the expected distribution. The arrow shows the significance of A1742−294 detection.

analysis. In the 1992 fall observations the flux from A1742−294 in the 35–100 keV band was found to be at the level of 31 ± 5.4 mcrab, corresponding to the luminosity $\approx 3 \times 10^{36}$ ergs s^{-1} (assuming 8.5 kpc distance). During other periods of observation in 1990 spring–1993 spring, the source has not been significantly detected with typical upper limit (averaged over each period) less than ≈ 15 mcrab (3 σ). During observations in 1993 fall the source was again detected by SIGMA. The 1993 fall observations suffer from the presence of a very bright source, GRS 1716−29, in the SIGMA field of view, and detailed analysis of the data on weak sources (like A1742−294) will be published elsewhere.

The light curve of A1742−294 in the 35–100 keV band obtained in individual sessions in 1992 fall is shown in Figure 5. The individual points of Figure 5 are consistent with the assumption of the constant 35–100 keV flux. The hard state lasted more than ≈ 10 days, i.e., many orders of magnitude longer than any characteristic time of the inner part of the accretion disk. Hence transition to the hard state is caused by some changes outside the inner part of the accretion disk.

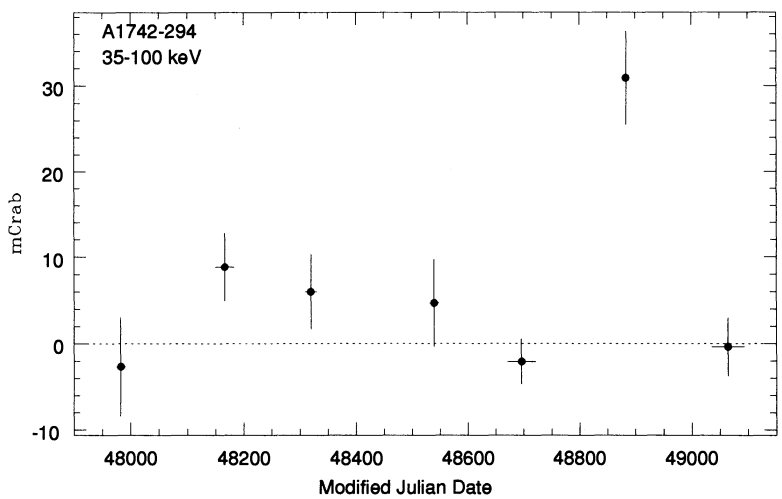

FIG. 4.—Light curve of the A1742−294 flux in the 35–100 keV band averaged over periods of observations in 1990 spring–1993 spring. Only the observations taken when the source was illuminating more than 70% of the detector area were used.

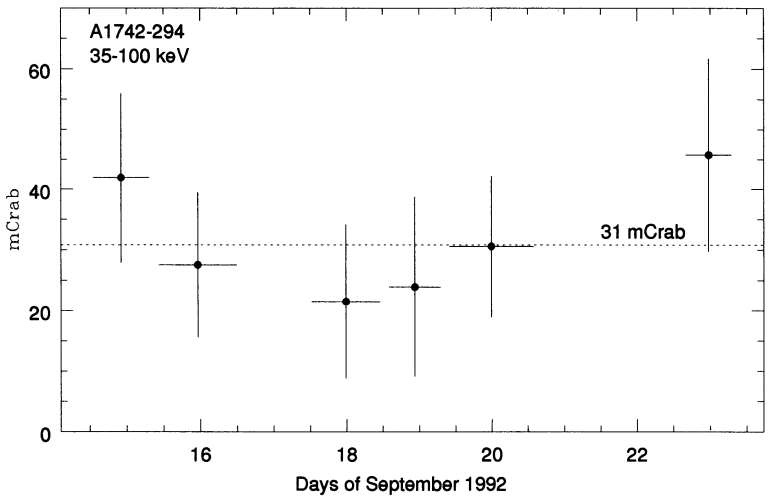

FIG. 5.—Light curve of the A1742−294 flux in the 35–100 keV band during the 1992 fall observations. The dashed line corresponds to the average level of 31 mcrab.

The best-fit parameters for power-law and optically thin plasma emission models in the 35–100 keV band are given in Table 2. Shown in Figure 6 is the spectrum of A1742−294 observed by SIGMA in 1992 fall. The spectrum observed by ART-P (averaged over 1990 fall observations) is also shown (from Pavlinsky et al. 1994). Both power-law and thermal emission of the optically thin plasma models provide equally good approximations of SIGMA data points. More complicated models are not required by the SIGMA data.

5. DISCUSSION

According to Spacelab 2 data (Skinner et al. 1987), A1742−294 luminosity in the 3–30 keV band is equal to 1.3×10^{37} ergs s^{-1} (for 8.5 kpc distance). The luminosity in the same band calculated using the fit to the averaged ART-P spectrum (Pavlinsky et al. 1994) is equal to 8×10^{36} ergs s^{-1}. Thus detection of the hard flux with luminosity ≈20%–30% of the typical value in the standard X-ray band does not in itself indicate strong changes in the total source luminosity.

As is seen from Figure 6, power-law and bremsstrahlung models do not differ strongly in the SIGMA band, but they predict very different fluxes at lower energies.

TABLE 2

PARAMETERS OF BEST-FIT POWER LAW AND THERMAL EMISSION OF OPTICALLY THIN PLASMA MODELS TO SIGMA 35–200 keV BAND DATA[a]

Model	A1742−294	1E 1740.7−2942
Power Law		
Photon index	3.1 ± 0.5	1.9 ± 0.1
F_{100}[b] (10^{-6} photons cm^{-2} s^{-1} keV^{-1})	9.2 ± 4	83 ± 4
χ^2 (dof)	31.8(38)	60.1(38)
Bremsstrahlung		
Temperature (keV)	41 ± 17	152 ± 30
F_{100}[b] (10^{-6} photons cm^{-2} s^{-1} keV^{-1})	9.2 ± 4	86 ± 4
χ^2 (dof)	31.4(38)	54.8(38)

[a] Errors are 68% confidence intervals for a single parameter of interest (Avni 1976).

[b] F_{100} = flux at 100 keV.

5.1. *Power Law*

In most of the ART-P observations in 1990 spring–1992 spring, the source flux in the 8–20 keV band was at the level of 20–40 mcrab. The brightest state, ≈70 mcrab, in this band was observed on 1991 September 3 (Pavlinsky et al. 1994). Extrapolation of the SIGMA best-fit power-law approximation of the

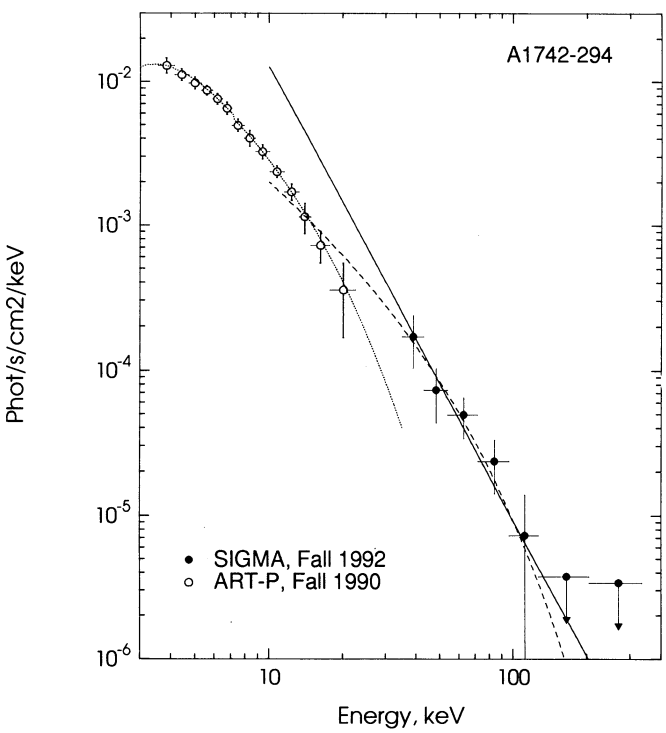

FIG. 6.—Spectrum of A1742−294 obtained by SIGMA during 1992 fall observations (*filled circles*). Upper limits are 1 σ values. The spectrum obtained by the ART-P telescope in the standard X-ray band (averaged over 1990 fall observations) is shown by open circles. The dotted line shows the bremsstrahlung approximation ($kT = 8$ keV) of the ART-P spectrum. Solid and long-dashed lines correspond to power-law and bremsstrahlung models (the best fit to 35–200 keV data points). The ART-P data are taken from Pavlinsky et al. (1994).

35–200 keV data (Table 1) to 10 keV corresponds to a rather high level of 150–200 mcrab. The all-sky monitor WATCH on broad *Granat* detected strong activity (in the 8–20 keV range) from the region of A1742−294 in 1992 fall, although an angular resolution $\sim 2°$ does not allow one to resolve the possible contribution of A1742−294 from nearby sources (Lapshov et al. 1994). Hence an outburst seen by SIGMA in hard X-rays is possibly accompanied by an increase in the standard X-ray flux. If the flux measured by WATCH is indeed related to A1742−294, it means that a power-law approximation with the photon index ≈ 3 can be extended down to the standard X-ray band.

5.2. *Optically Thin Thermal Emission*

The value of the temperature $T_e \sim 40$ keV found under assumption of the thermal bremsstrahlung model (see Table 2) is much higher than $T_e \sim 8$ keV found by ART-P during 1990 observations in the standard X-ray band (Pavlinsky et al. 1994). The assumption that SIGMA detection of A1742−294 is only due to the increase of the source brightness (i.e., the shape of the spectrum corresponds to ≈ 8 keV bremsstrahlung) gives $\chi^2 = 44.2$ for 39 dof versus $\chi^2 = 31.8$ for 38 dof at the best-fit $T_e = 41$ keV. On the other hand, assumption of 41 keV bremsstrahlung over the entire X-ray band would predict a flux at 10 keV at the level of ≈ 20–30 mcrab. If this model is valid, then WATCH detection of a ≈ 200 mcrab source within $\sim 2°$ from A1742−294 is not associated with A1742−294, or an additional soft component in the A1742−294 spectrum is present.

In any case, detection of A1742−294 above 35 keV by SIGMA indicates that a spectrum in the hard state is not consistent with the extrapolation of a spectrum observed during other periods in the standard X-ray band.

Detection of type I X-ray bursts from A1742−294 firmly identifies this source as a neutron star binary. The X-ray spectra of the neutron star binaries sharply decline toward high energies, so that usually they can hardly be detected above 30 keV. In particular, SIGMA did not detect significant emission from such very bright objects in the standard X-ray band as GX5−1, GX3+1, GX9+1, etc. However, during *Granat*/SIGMA observations of the GC region, evidence for variable activity of X-ray bursters above 30 keV has been found for KS 1731−260 (Barret et al. 1991), X1724−308/Terzan 2 (Barret et al. 1992), GX354−0 (Claret et al. 1994), and A1742−294 (this paper). The extrapolation of their spectra typically observed in standard X-rays to the SIGMA energy band would predict very low values of flux, and spectral changes (or the presence of additional hard components) are required in order to explain these detections. It was recently found by van Paradijs & van der Klis (1994) that weaker (lower luminosity) low-mass X-ray binaries have on average harder X-ray spectra. If individual sources also exhibit similar behavior, then one can expect the decrease of the source luminosity simultaneously with hardening of the spectrum. Power-law and bremsstrahlung models (see above) predict luminosities in the 3–100 keV band of 5.7×10^{37} and 9.4×10^{36} ergs s^{-1} respectively. These values should be compared with luminosities found by Spacelab 2 and ART-P. Association of high WATCH flux with A1742−294 would argue in favor of high luminosity in the hard state and would place this source far apart from the trend found by van Paradijs & van der Klis (1994). Bremsstrahlung fit predicts a rather flat spectrum in the standard X-ray band, and its luminosity can be used as the crude lower limit on the source luminosity during the hard state. This value is comparable to the luminosity found by ART-P and is only a factor of 1.4 less than the luminosity measured by Spacelab 2. The requirement of a substantial decrease of luminosity in the hard state would mean that the spectrum in the standard X-ray band is flatter than that of the bremsstrahlung fit.

5.3. *Comptonization Model*

The Comptonization of low-frequency photons on the hot electrons is considered as a plausible mechanism of the formation of hard X-ray components in the spectra of compact Galactic sources. Instead of the usually used pair of optical depth τ_T and electron temperature T_e, one can define the model by the enhancement factor and T_e. The enhancement factor characterizes the ratio of the energy release in the Comptonization region to the soft photon flux entering the region. The low-energy ($E \ll T_e$) part of the spectrum can be described by the steep or hard power law for low and high enhancement factors, respectively. It was suggested that neutron star binaries have steep spectra because of the presence of the neutron star surface close to the region of formation of the hard spectrum (see, e.g., the calculations of Sunyaev & Titarchuk 1989). The neutron star surface reprocesses a significant fraction of hard X-ray flux from the Comptonization region and returns it in the form of soft photons. As a result, the enhancement factor cannot be high, and the spectrum should be steep in both hard and standard X-ray bands. Unfortunately, power-law and bremsstrahlung approximations (see above) demonstrate that SIGMA data alone can be understood either as the continuation of a steep power law (i.e., low enhancement factor and

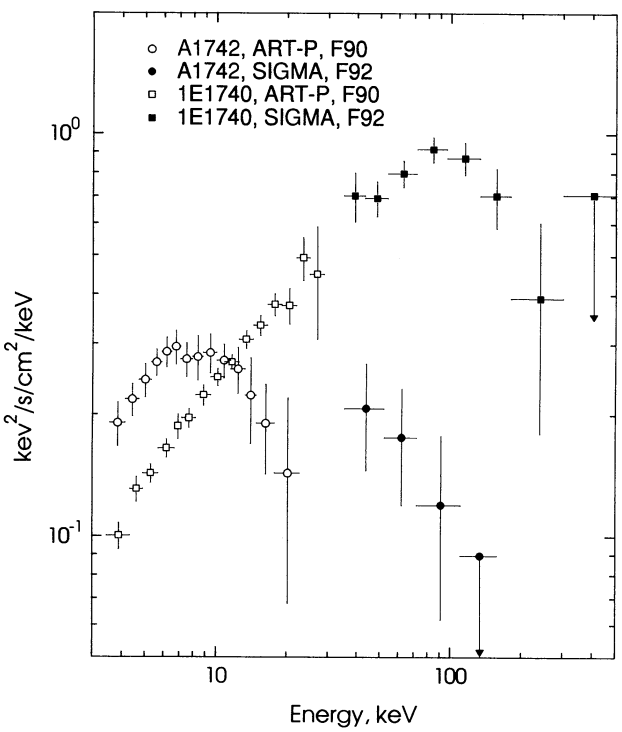

FIG. 7.—Plots of νF_ν for A1742−294 and 1E 1740.7−2942 spectra observed by SIGMA in 1992 fall. The spectra of A1742−294 and 1E 1740.7−2942 in the standard X-ray band from ART-P spectra (averaged over 1990 fall observations) are also shown (the data are from Pavlinsky et al. 1994).

high temperature) or as the cutoff part of a somewhat harder spectrum (high enhancement factor and low electron temperature). Simultaneous observations at low energies are required in order to distinguish between these two possibilities. The association of flux measured by WATCH with the source is consistent with the former assumption. If instead the spectrum in the standard X-ray band was hard (as would follow from the requirement of low luminosity), then one can conclude that reprocessing of hard radiation by the neutron star surface does not play a crucial role in the formation of the hard component in the spectrum of A1742−294, at least during the hard state of the source.

5.4. *Comparison with 1E 1740.7−2942*

The broadband spectra of bright Galactic sources observed by *Mir-Kvant* instruments (Sunyaev et al. 1991e) demonstrate that power-law components in the spectra of black hole candidates are remarkably harder than the spectra of neutron star binaries. Although SIGMA results indicate the presence of hard X-rays from the latter sources (at least during a fraction of time), their spectra are softer than typical spectra of black hole candidates. There is one possible exception to this rule in SIGMA data: a very hard spectrum of Terzan 2 observed by SIGMA in 1990 spring (Barret et al. 1992). It is possible, however, that there are two X-ray sources in this globular cluster, and hard X-rays detected in 1990 spring are not associated with a well-known burster, X1742−308. In later observations in 1990–1993 the spectrum of the Terzan 2 region was much softer (Gilfanov et al. 1994; Goldwurm et al. 1994).

One of the nearby (to A1742−294) sources, 1E 1740.7−2942, is considered as a black hole candidate because of its hard spectrum, resembling that of Cyg X-1 (Sunyaev et al. 1991c, d). This source was observed simultaneously with A1742−294 in 1992 fall (Cordier et al. 1993). The best-fit parameters for the 1E 1740.7−2942 are given in Table 2. Approximation of the 1E 1740.7−2942 spectra by a bremsstrahlung model requires the temperature ~ 150 keV, i.e., much higher than that for A1742−294. Even more convincing is the comparison of A1742−294 and 1E 1740.7−2942 spectra in units of $\mathrm{keV}^2\ \mathrm{s}^{-1}\ \mathrm{cm}^{-2}\ \mathrm{keV}^{-1}$ (i.e., luminosity per decade of energy), shown in Figure 7. One can see that for 1E 1740.7−2942, the νF_ν spectrum peaks at ≈ 100 keV, while for A1742−294 the maximum on the spectrum is in any case at an energy below ≈ 30 keV. If a power law with photon index ≈ 3 extends toward lower energies, the maximum of the νF_ν spectrum will also be at low energies.

This work was supported in part by Russian Fundamental Research Foundation grant 93-02-17166.

REFERENCES

Avini, Y. 1976, ApJ, 210, 642
Barret, D., et al. 1991, ApJ, 379, L21
———. 1992, ApJ, 394, 615
Claret, A., et al. 1994, ApJ, 423, 436
Cordier, B., et al. 1993, A&A, 275, L1
Fenimore, E. E., & Cannon, T. M. 1981, Appl. Optics, 20, 1858
Gilfanov, M., et al. 1994, in Proc. NATO Workshop (Dordrecht: Kluwer), in press
Goldwurm, A., et al. 1994, in AIP Conf. Proc. 304, Second Compton Symp., ed. C. Fichtel, N. Gehrels, & J. Norris (New York: AIP), 421
Jernigan, J. G., Bradt, H. V., Doxsey, R. E., Dower, R. G., McClintock, J. E., & Apparao, K. M. V. 1978, Nature, 272, 701
Kawai, N., Fenimore, E. E., Middleditch, J., Cruddace, R. G., Fritz, G. G., Snyder, W. A., & Ulmer, M. P. 1988, ApJ, 330, 130
Lapshov, I., et al. 1994, in preparation
Lewin, W., et al. 1976, MNRAS, 177, 83
Paul, J., et al. 1991, Adv. Space Res., 11, 289
Pavlinsky, M. N., Grebenev, S. A., & Sunyaev, R. A. 1994, ApJ, 425, 110
Proctor, R. J., Skinner, G. K., & Willmore, A. P. 1978, MNRAS, 185, 745
Skinner, G. K., Willmore, A. P., Eyles, C. J., Bertram, D., & Church, M. J. 1987, Nature, 330, 544
Sunyaev, R., & Titarchuk, L. 1989, in Proc. 23d ESLAB Symp., ed. J. Hunt & B. Battrick (ESA SP-296; Paris: ESA), 1, 627
Sunyaev, R., et al. 1991a, Soviet Astron. Lett., 17, 99
———. 1991b, Soviet Astron. Lett., 17, 126
———. 1991c, A&A, 247, L29
———. 1991d, ApJ, 383, L49
———. 1991e, Soviet Astron. Lett., 17, 975
Watson, M. G., Willingale, R., Grindlay, J. E., & Hertz, P. 1981, ApJ, 250, 142
Wilson, A. M., Carpenter, G. F., Eyles, C. J., Skinner, G. K., & Willmore, A. P. 1977, ApJ, 215, L111
van Paradijs, J., & van der Klis, M. 1994, A&A, 281, L17